

## EARLY SPECTROSCOPIC IDENTIFICATION OF SN 2008D<sup>1</sup>

D. MALESANI<sup>2</sup>, J. P. U. FYNBO<sup>2</sup>, J. HJORTH<sup>2</sup>, G. LELOUDAS<sup>2</sup>, J. SOLLERMAN<sup>2,3</sup>, M. D. STRITZINGER<sup>4,2</sup>, P. M. VREESWIJK<sup>2</sup>, D. J. WATSON<sup>2</sup>, J. GOROSABEL<sup>5</sup>, M. J. MICHALOWSKI<sup>2</sup>, C. C. THÖNE<sup>2</sup>, T. AUGUSTEIJN<sup>6</sup>, D. BERSIER<sup>7</sup>, P. JAKOBSSON<sup>8</sup>, A. O. JAUNSEN<sup>9</sup>, C. LEDOUX<sup>10</sup>, A. J. LEVAN<sup>11</sup>, B. MILVANG-JENSEN<sup>2</sup>, E. ROL<sup>12</sup>, N. R. TANVIR<sup>12</sup>, K. WIERSEMA<sup>12</sup>, D. XU<sup>2</sup>, L. ALBERT<sup>13</sup>, M. BAYLISS<sup>14,15</sup>, C. GALL<sup>2</sup>, L. F. GROVE<sup>2</sup>, B. P. KOESTER<sup>14,15</sup>, E. LEITET<sup>16</sup>, T. PURSIMO<sup>6</sup>, I. SKILLEN<sup>17</sup>

*Draft version November 6, 2018*

### ABSTRACT

SN 2008D was discovered while following up an unusually bright X-ray transient (XT) in the nearby spiral galaxy NGC 2770. We present early optical spectra (obtained 1.75 days after the XT) which allowed the first identification of the object as a supernova (SN) at redshift  $z = 0.007$ . These spectra were acquired during the initial declining phase of the light curve, likely produced in the stellar envelope cooling after shock breakout, and rarely observed. They exhibit a rather flat spectral energy distribution with broad undulations, and a strong, W-shaped feature with minima at 3980 and 4190 Å (rest frame). We also present extensive spectroscopy and photometry of the SN during the subsequent photospheric phase. Unlike SNe associated with gamma-ray bursts, SN 2008D displayed prominent He features and is therefore of Type Ib.

*Subject headings:* supernovae: individual (SN 2008D)

### 1. OBSERVATIONS OF SN 2008D

On 2008 January 9.56 UT, while observing the supernova (SN) 2007uy in the nearby spiral galaxy NGC 2770 ( $z = 0.007$ ), the X-Ray Telescope onboard *Swift* detected a bright X-ray transient (XT), with a peak luminosity of  $6 \times 10^{43}$  erg s<sup>-1</sup> and a duration of about 10 minutes

<sup>1</sup> Partly based on observations made with ESO telescopes at the La Silla Paranal Observatory under program 080.D-0526, with the Nordic Optical Telescope, operated on the island of La Palma jointly by Denmark, Finland, Iceland, Norway, and Sweden, and with the United Kingdom Infrared Telescope, which is operated by the Joint Astronomy Centre on behalf of the Science and Technology Council of the UK.

<sup>2</sup> Dark Cosmology Centre, Niels Bohr Institute, University of Copenhagen, Juliane Maries vej 30, 2100 Copenhagen Ø, Denmark

<sup>3</sup> Department of Astronomy, Stockholm University, 10691 Stockholm, Sweden

<sup>4</sup> Las Campanas Observatory, Carnegie Institute of Science, Colina el Pino Casilla 601, La Serena, Chile

<sup>5</sup> Instituto de Astrofísica de Andalucía (IAA-CSIC), Apartado 3004, 18080 Granada, Spain

<sup>6</sup> Nordic Optical Telescope, Apartado 474, 38700 Santa Cruz de La Palma, Spain

<sup>7</sup> Astrophysics Research Institute, Liverpool John Moores University, Twelve Quays House, Egerton Wharf, Birkenhead, CH41 1LD, UK

<sup>8</sup> Centre for Astrophysics and Cosmology, Science Institute, University of Iceland, Dunhagi 5, 107 Reykjavík, Iceland

<sup>9</sup> Institute of Theoretical Astrophysics, University of Oslo, P.O. Box 1029, Blindern, 0315 Oslo, Norway

<sup>10</sup> European Southern Observatory, Avenida Alonso de Cordova 3107, Casilla 19001, Vitacura, Santiago, Chile

<sup>11</sup> Department of Physics, University of Warwick, Coventry CV4 7AL, UK

<sup>12</sup> Department of Physics and Astronomy, University of Leicester, Leicester, LE1 7RH, UK

<sup>13</sup> Canada-France-Hawaii Telescope Corporation, 65-1238 Mamalahoa Highway, Kamuela, HI 96743, USA

<sup>14</sup> Department of Astronomy and Astrophysics, University of Chicago, 5640 South Ellis Avenue, Chicago, IL 60637, USA

<sup>15</sup> Kavli Institute for Cosmological Physics, 5640 South Ellis Avenue, Chicago, IL 60637, USA

<sup>16</sup> Department of Physics and Astronomy, Uppsala University, Box 515, SE-751 20 Uppsala, Sweden

<sup>17</sup> Isaac Newton Group, Apartado 321, 38700 Santa Cruz de La Palma, Canary Islands, Spain

(Soderberg et al. 2008a). Its power-law spectrum and light curve shape were reminiscent of gamma-ray bursts (GRBs) and X-ray flashes, but the energy release was at least 2 orders of magnitude lower than for typical and even subluminal GRBs, also allowing for beaming (e.g., Amati 2006; Ghirlanda et al. 2007). The discovery of the XT prompted the search for, and discovery of, an optical counterpart (Deng & Zhu 2008; Valenti et al. 2008a).

We performed spectroscopy of the source as soon as possible, starting 1.75 days after the XT, using the FORS2 spectrograph on the ESO Very Large Telescope (VLT). Subsequent spectroscopic monitoring of the object was carried out at the Nordic Optical Telescope (NOT) and the William Herschel Telescope (WHT). All spectra have been reduced using standard techniques. On January 18.22 UT (8.65 days after the XT) we secured a high-resolution spectrum using the UVES instrument on the VLT. For this observation, we adopted the ESO CPL pipeline (v3.3.1), and flux calibration was performed using the master response curves. The observing log of the spectra is reported in Table 1.

Imaging observations were conducted using the NOT, the VLT, the Liverpool Telescope (LT) and the United Kingdom Infrared Telescope (UKIRT). Image reduction was carried out using standard techniques. For photometric calibration, we observed optical standard star fields on five different nights, and defined a local sequence in the NGC 2770 field. In the near-infrared we used Two Micron All Sky Survey stars as calibrators. Magnitudes were computed using small apertures, and subtracting the background as measured in an annulus around the SN position. The contribution from the underlying host galaxy light was always negligible, as also apparent from archival Sloan Digital Sky Survey images. Our photometric results are listed in Table 2.

One of our spectra covers the nucleus of NGC 2770, allowing a precise measurement of its redshift:  $z = 0.0070 \pm 0.0009$ . This is slightly larger than the value listed in the NASA Extragalactic Database ( $z = 0.0065$ ).

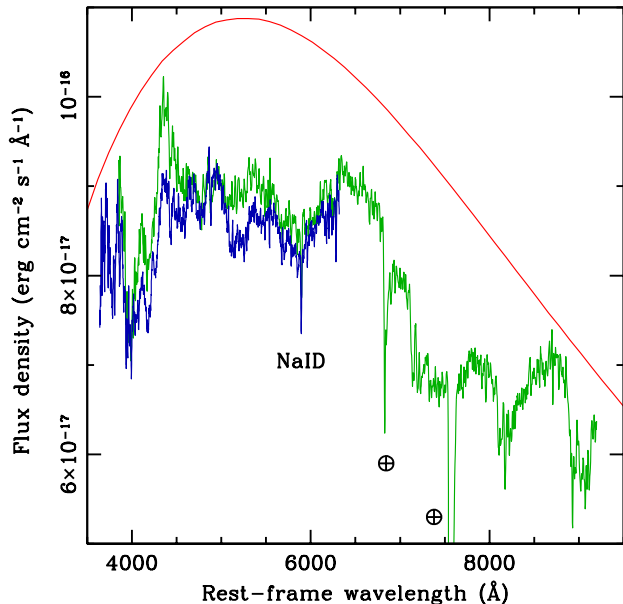


FIG. 1.— Our two earliest spectra obtained 1.75 days after the XT, when the cooling envelope emission was dominating the observed light. The spectra cover the wavelength ranges 3600–6300 Å (grism 600B, blue curve) and 3800–9200 Å (grism 300V, green curve). For comparison, the red line shows a blackbody spectrum with temperature  $T = 15,000$  K, reddened assuming  $E(B - V) = 0.8$  mag (Section 2.3). The Na I D narrow absorption from the interstellar medium in NGC 2770 is also noted, as well as the two strong telluric features (marked with ‘⊕’).

For  $H_0 = 71$  km s $^{-1}$  Mpc $^{-1}$ , the luminosity distance is 29.9 Mpc.

## 2. RESULTS

### 2.1. The Early Spectrum of SN 2008D

Our first optical spectrum of the transient source (Figure 1) exhibits Na I D absorption lines at  $z = 0.0070$ , thus establishing its extragalactic nature. Broad features are also apparent across the whole spectrum (FWHM =  $(1-3) \times 10^4$  km s $^{-1}$ ), which led us to identify the object as a core-collapse SN (Malesani et al. 2008). Soderberg et al. (2008a,b) describe nearly simultaneous spectra as featureless, probably due to their smaller covered wavelength range (4500–8000 Å). Modjaz et al. (2008a) report features consistent with those in our data.

We initially classified the SN as a very young Type Ib/c, based on the absence of conspicuous Si and H lines (Malesani et al. 2008). As the spectrum is among the earliest observed for any SN, comparable only to the very first spectrum of SN 1987A (Menziés et al. 1987), there is no obvious resemblance with known SN spectra. It is notable, however, that the earliest spectrum of the Type-Ic SN 1994I was essentially flat with broad, low-amplitude undulations (though the covered wavelength range was limited; Filippenko et al. 1995). Early spectra, also mostly featureless, are available for the H-rich Type-IIP SN 2006bp (Quimby et al. 2006). Dessart et al. (2008) interpret them in terms of high temperature and ionization.

A striking feature in the spectrum is a conspicuous W-shaped absorption with minima at 3980 and 4190 Å (rest frame). It was detected using two different instrument

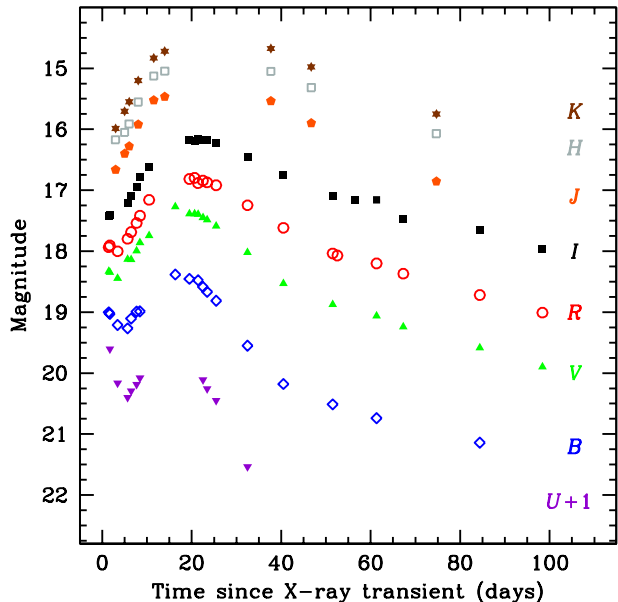


FIG. 2.— Optical and near-infrared light curves of SN 2008D. The data points are not corrected for extinction. Error bars are smaller than symbols and have been omitted.

setups (Figure 1), and also reported by Modjaz et al. (2008a). If interpreted as due to P Cyg profiles, the inferred expansion velocity is  $\sim 15,000$  km s $^{-1}$ , computed from the position of the bluest part compared to the peak. Its origin is unclear, although, following Quimby et al. (2007), Modjaz et al. (2008a) propose that it is due to a combination of C III, N III, and O III. Interpreting the broad absorption at  $\sim 5900$  Å as Si II  $\lambda\lambda$  6347, 6371, some ejecta reached  $\sim 22,000$  km s $^{-1}$ . Such large velocities have been seen only in broad-lined (BL) Type-Ic SNe, at significantly later stages (Patat et al. 2001; Hjorth et al. 2003; Mazzali et al. 2006).

### 2.2. The Photospheric Phase

Figure 2 shows the optical and near-infrared light curves of SN 2008D. In the first days after the XT, the flux dropped faster in the bluer bands, with the color becoming progressively redder. This can be interpreted as due to the stellar envelope cooling after the shock breakout (Soderberg et al. 2008a). Our first spectra were taken during this stage, before energy deposition by radioactive nuclei became dominant, hence the physical conditions of the emitting material might be different than later. We note that the W-shaped absorption discussed in Section 2.1 was no longer visible from 3.5 days after the XT onward (Fig. 3).

The later spectra, acquired during the radioactivity-powered phase and extending over more than two months in time, established SN 2008D as a Type-Ib SN (Modjaz et al. 2008b). From January 17 and onward unambiguous He lines are observed (Figure 3), consistent with other reports (Modjaz et al. 2008a; Valenti et al. 2008b; Soderberg et al. 2008a; Tanaka et al. 2008; Mazzali et al. 2008). In Figure 4, we plot the velocities at maximum absorption of a few transitions determined using the SYNOW code (Fisher et al. 1999). For comparison, we also plot the Si II velocity of

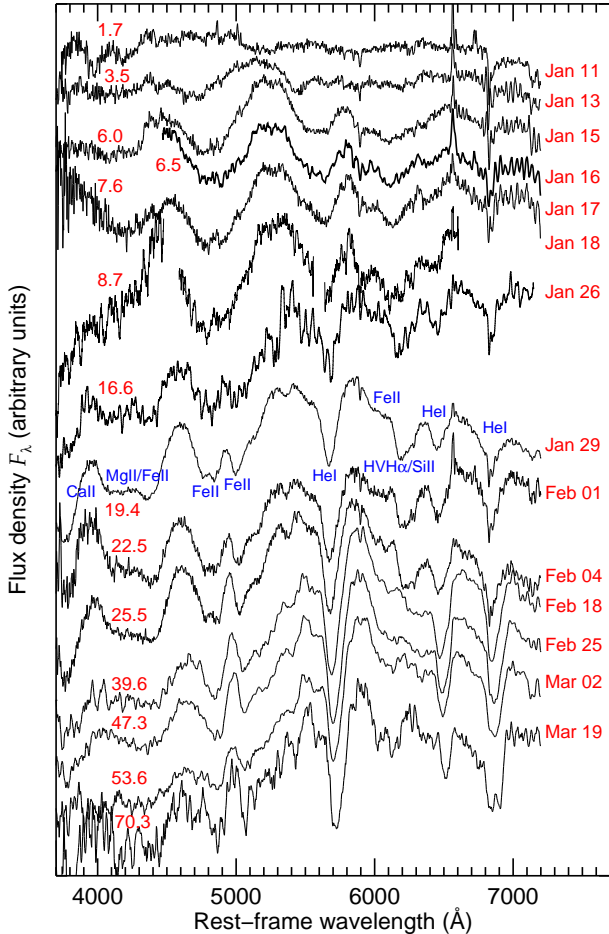


FIG. 3.— Spectral evolution of SN 2008D from 1.75 days to 7 weeks after explosion. On the left, the time in days since the XT is noted. The spectrum marked as “Jan 16” is the average of those taken on January 15.95 and 16.26 UT. Close to the January 29 track we have indicated the most likely identification of the main features (HVH $\alpha$  stands for “high-velocity H $\alpha$ ”). The narrow emission line at 6560  $\text{\AA}$  is residual H $\alpha$  from the SN host galaxy. The He I feature around 6800  $\text{\AA}$  is affected by the B-band atmospheric absorption.

the BL SN 1998bw (Patat et al. 2001) and of the normal Type-Ic SN 1994I (Sauer et al. 2006), showing that the velocities of SN 2008D are lower than those of BL SNe.

### 2.3. Dust Extinction

It follows from the detection of strong Na I D with an equivalent width (EW) of 1.3  $\text{\AA}$  that the extinction toward SN 2008D is substantial in NGC 2770. Our best estimate of the reddening comes from comparing the colors of SN 2008D with those of stripped-envelope SNe, which have  $V - R \approx R - I \approx 0.1$  around maximum (e.g., Folatelli et al. 2006; Richmond et al. 1996; Galama et al. 1998). The resulting reddening is  $E(B - V) = 0.8$  mag, corresponding to an extinction  $A_V = 2.5$  mag (using the extinction law by Cardelli et al. 1989 with  $R_V = 3.1$ ).

A large dust content is supported by absorption features in our high-resolution spectrum (see also Soderberg et al. 2008a). The Na I D1 absorption line indicates a multicomponent system, spanning a velocity range of 43  $\text{km s}^{-1}$ , which sets a lower limit  $E(B - V) > 0.2$  mag (Munari & Zwitter 1997, their Figure 4). The

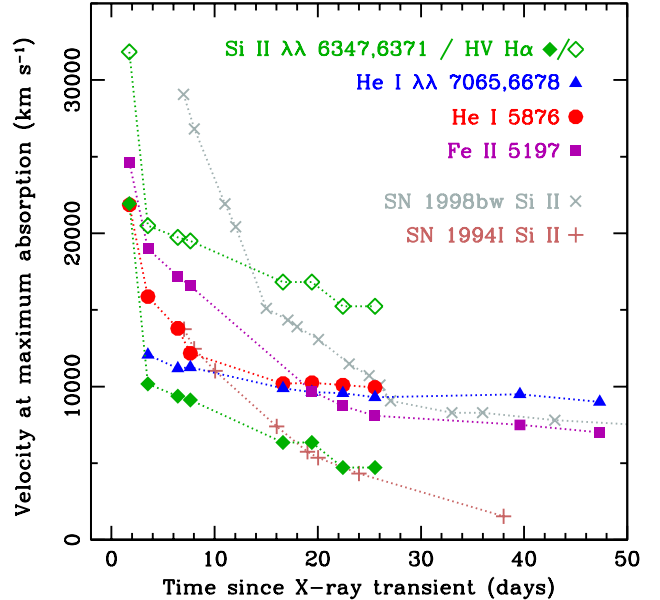


FIG. 4.— Velocity at maximum absorption of several transitions computed with SYNOW. Diamonds indicate the velocity for the 6200  $\text{\AA}$  line if interpreted as Si II (filled symbols) or HV H $\alpha$  (open symbols). The latter interpretation is unlikely due to the lack of corresponding H $\beta$  (see also Tanaka et al. 2008). SN 2008D shows velocities lower than the prototypical hypernova SN 1998bw (Patat et al. 2001) and comparable to SN 1994I (Sauer et al. 2006).

Na I D versus  $E(B - V)$  relation for SNe (Turatto et al. 2003) suggests  $0.2 \text{ mag} \lesssim E(B - V) \lesssim 0.6 \text{ mag}$ . Diffuse interstellar bands (DIBs) are also detected at 5781.2, 5797.8, and 6283.9  $\text{\AA}$  (rest frame). Their EWs suggest  $0.5 \text{ mag} \lesssim E(B - V) \lesssim 2 \text{ mag}$  (Cox et al. 2005). A dusty environment has been directly revealed through millimeter imaging of NGC 2770 (Gorosabel et al. 2008). Last, the hydrogen column density in the X-ray spectrum of the XT is  $N_{\text{H}} = 6.9^{+1.8}_{-1.5} \times 10^{21} \text{ cm}^{-2}$  (assuming Solar abundances; Soderberg et al. 2008a). The gas-to-dust ratio is  $N_{\text{H}}/A_V = 2.8 \times 10^{21} \text{ cm}^{-2} \text{ mag}^{-1}$ , close to the Galactic value  $1.7 \times 10^{21} \text{ cm}^{-2} \text{ mag}^{-1}$  (Predehl & Schmitt 1995).

### 3. DISCUSSION

The precise explosion epoch is so far only known for a few Type-II SNe, thanks to either the detection of the neutrino signal (SN 1987A; Hirata et al. 1987; Bionta et al. 1987) or of the UV flash by *Galaxy Evolution Explorer* (Shawinski et al. 2008; Gezari et al. 2008), and for BL Type-Ic SNe associated with GRBs (e.g., Galama et al. 1998; Hjorth et al. 2003; Stanek et al. 2003; Campana et al. 2006). SN 2008D is the first Type-Ib SN with a precisely constrained explosion epoch, since the XT is expected to occur less than 1 hr after the stellar collapse (Li 2007; Waxman et al. 2007). The nature of the XT — shock breakout versus relativistic ejecta — is still debated (Soderberg et al. 2008a; Xu et al. 2008; Li 2008; Mazzali et al. 2008; Chevalier & Fransson 2008), thus it is unclear whether this phenomenon is common.

The light-curve evolution of SN 2008D is very similar to that of SN 1999ex (Stritzinger et al. 2002). The initial fading can be interpreted as due to the enve-

lope cooling through expansion following the initial X-ray/UV flash (Stritzinger et al. 2002; Campana et al. 2006; Soderberg et al. 2008a). The subsequent rebrightening is due to the energy released by radioactive material in the inner layers and gradually reaching the optically thin photosphere.

From our *UBVRI* data, we constructed the bolometric light curve of SN 2008D (Figure 5). For comparison we also show the two other He-rich SNe caught during the early cooling phase: SN 1993J (Richmond et al. 1994) and SN 1999ex (Stritzinger et al. 2002). Strikingly, the three SNe had very similar light curves during the photospheric phase. Given its peak luminosity, SN 2008D synthesized about  $0.09M_{\odot}$  of  $^{56}\text{Ni}$  based on Arnett's rule (Arnett 1982). The emission during the early cooling phase, however, varied substantially for the three SNe (seen only in *U* for SN 1999ex). Furthermore, significant radiation may be emitted blueward of the *U* band during this early phase, so that the bolometric values may be underestimated.

SN 2008D has different properties from the SNe associated with GRBs, namely the presence of He in the ejecta, a lower peak luminosity ( $\approx 1.5$  mag), lower expansion velocities (a factor of  $\approx 2$ ), and lower  $^{56}\text{Ni}$  mass (a factor of  $\approx 5$ ). The SN environment is also unlike that of GRBs (Soderberg et al. 2008a; Thöne et al. 2008). Whether these two kinds of high-energy transients are separate

phenomena or form a continuum is unclear. Addressing this issue will require theoretical modeling and an enlarged sample. The discovery of a short-lived XT associated with an ordinary Type-Ib SN opens the possibility of accessing the very early phases of ordinary SNe, which will provide new insights into SN physics. Future X-ray sky-scanning experiments, such as Lobster or eROSITA, may turn out, rather unexpectedly, ideally suited to examine this issue, alerting us to the onset of many core collapse SNe.

The Dark Cosmology Centre is supported by the DNRF. J.G. is supported by the Spanish research programs AYA2004-01515 and ESP2005-07714-C03-03 and P.M.V. by the EU under a Marie Curie Intra-European Fellowship, contract MEIF-CT-2006-041363. P.J. acknowledges support by a Marie Curie European Reintegration Grant within the 7th European Community Framework Program under contract number PERG03-GA-2008-226653, and a Grant of Excellence from the Icelandic Research Fund. We thank M. Modjaz and M. Tanaka for discussion, and the observers at VLT, NOT, WHT, UKIRT, in particular A. Djupvik, S. Niemi, A. Somero, T. Stanke, J. Telting, H. Uthas, and C. Villforth.

#### REFERENCES

- Amati, L. 2006, MNRAS, 372, 233  
 Arnett, W. D. 1982, ApJ, 253, 785  
 Bionta, R. M., et al. 1987, Phys. Rev. Lett., 58, 1494  
 Campana, S., et al. 2006, Nature, 442, 1008  
 Cardelli, J. A., Clayton, G. C., & Mathis, J. S. 1989, ApJ, 345, 245  
 Chevalier, R., & Fransson, C. 2008, ApJ, 683, L135  
 Cox, N. L. J., Kaper, L., Foing, B. H., & Ehrenfreund, P. 2005, A&A, 438, 187  
 Deng, J., & Zhu, Y. 2008, GCN Circ. 7160  
 Dessart, L., et al. 2008, ApJ, 675, 644  
 Filippenko, A. V., et al. 1995, ApJ, 450, L11  
 Fisher, A., Branch, D., Hatano, K., & Baron, E. 1999, MNRAS, 304, 67  
 Folatelli, G., et al. 2006, ApJ, 641, 1039  
 Galama, T. J., et al. 1998, Nature, 395, 670  
 Gezari, S., et al. 2008, ApJ, 683, L131  
 Ghirlanda, G., Nava, L., Ghisellini, G., & Firmani, C. 2007, A&A, 466, 127  
 Gorosabel, J., et al. 2008, ApJL, arXiv:0810.4333, submitted  
 Hjorth, J., et al. 2003, Nature, 423, 847  
 Hirata, K., et al. 1987, Phys. Rev. Lett., 58, 1490  
 Li, L.-X. 2007, MNRAS, 375, 240  
 Li, L.-X. 2008, MNRAS, 388, 603  
 Malesani, D., et al. 2008, GCN Circ. 7169  
 Mazzali, P. A., et al. 2006, Nature, 442, 1011  
 Mazzali, P. A., et al. 2008, Science, 321, 1185  
 Menzies, J. W., et al. 1987, MNRAS, 227, 39  
 Modjaz, M., Li, W., Butler, N., et al. 2008a, ApJ, submitted (arXiv:0805.2201)  
 Modjaz, M., Chornock, R., Foley, R. J., Filippenko, A. V., Li, W., & Stringfellow, G. 2008b, CBET 1221  
 Munari, U., & Zwitter, T. 1997, A&A, 318, 269  
 Patat, F., et al. 2001, ApJ, 555, 900  
 Predehl, P., & Schmitt, J. H. M. M. 1995, A&A, 293, 889  
 Quimby, R. M., Wheeler, J. C., Höflich, P., Akerlof, C. W., Brown, P. J., & Rykoff, E. S. 2006, ApJ, 666, 1093  
 Quimby, R. M., Aldering, G., Wheeler, J. C., Höflich, P., Akerlof, C. W., & Rykoff, E. S. 2007, ApJ, 668, L99

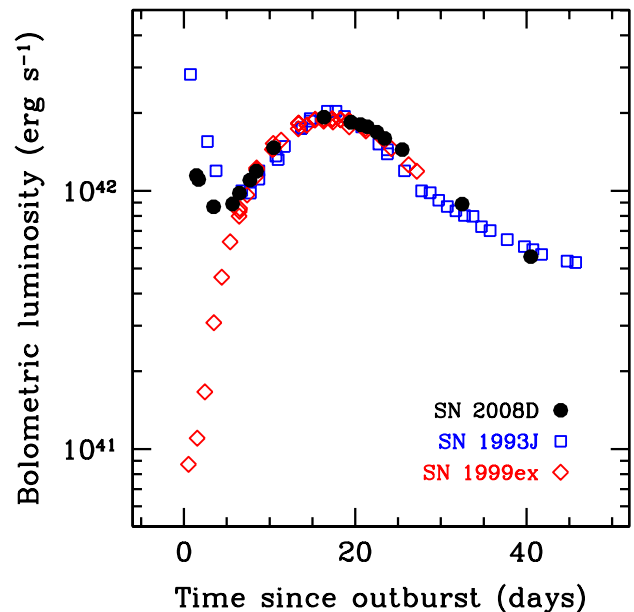


FIG. 5.— Bolometric light curves of SN 2008D (Type Ib), SN 1993J (Type Ib), and SN 1999ex (Type Ib). Extinctions corresponding to  $E(B - V) = 0.8, 0.19$  and  $0.30$  mag were assumed. The cooling envelope phase was visible only in the *U* band for SN 1999ex.

- Richmond, M. W., Treffers, R. R., Filippenko, A. V., Paik, Y., Leibundgut, B., Schulman, E., & Cox, C. V. 1994, AJ, 107, 1022  
 Richmond, M. W., et al. 1996, AJ, 111, 327  
 Sauer, D. N., Mazzali, P. A., Deng, J., Valenti, S., Nomoto, K., & Filippenko, A. V. 2006, MNRAS, 369, 1939  
 Schawinski, K., et al. 2008, Science, 321, 223

TABLE 1  
LOG OF SPECTROSCOPIC OBSERVATIONS. PHASES ARE COMPUTED RELATIVE TO  
THE XT ONSET.

Epoch (UT)	Phase (days)	Telescope/instrument	Exposure time (s)
Jan 11.31	1.75	VLT/FORS2+G300V	1 × 600
Jan 11.32	1.76	VLT/FORS2+G600B	1 × 900
Jan 13.07	3.51	NOT/ALFOSC+G4	3 × 1200
Jan 15.17	5.61	NOT/ALFOSC+G4	3 × 1200
Jan 15.95	6.39	NOT/ALFOSC+G4	1 × 1200
Jan 16.26	6.70	NOT/ALFOSC+G4	1 × 1200
Jan 17.20	7.64	NOT/ALFOSC+G4	3 × 1200
Jan 18.22	8.66	VLT/UVES+Dic#1	1 × 3600
Jan 26.15	16.59	WHT/ISIS+R300B/R316R	6 × 600
Jan 29.01	19.45	NOT/ALFOSC+G4	3 × 1200
Feb 01.02	53.46	NOT/ALFOSC+G4	2 × 900
Feb 04.05	56.49	NOT/ALFOSC+G4	2 × 900
Feb 18.15	70.59	NOT/ALFOSC+G4	3 × 1200
Feb 25.88	78.32	NOT/ALFOSC+G4	2 × 1500
Mar 02.18	112.62	NOT/ALFOSC+G4	3 × 1200
Mar 18.87	129.31	NOT/ALFOSC+G4	3 × 900

Soderberg, A. M., et al. 2008a, *Nature*, 453, 469  
Soderberg, A. M., Berger, E., Fox, D., Cucchiara, A., Rau, A.,  
Ofek, E., Kasliwal, M., & Cenko, S. B. 2008b, *GCN Circ.* 7165  
Stanek, K. Z., et al. 2003, *ApJ*, 591, L17  
Stritzinger, M., et al. 2002, *AJ*, 124, 2100  
Tanaka, M., et al. 2008, *ApJ*, arXiv:0807.1674, in press  
Thöne, C. C., Michalowski, M. J., Leloudas, G., Cox, N. L. J.,  
Fynbo, J. P. U., Sollerman, J., Hjorth, J., & Vreeswijk, P. M.  
2008, *ApJ*, arXiv:0807.0473, submitted  
Turatto, M., Benetti, S., & Cappellaro, E. 2003, *From Twilight to  
Highlight: The Physics of Supernovae*, ed. W. Hillebrandt & B.  
Leibundgut (Berlin: Springer), 200

Valenti, S., Turatto, M., Navasardyan, H., Benetti, S., &  
Cappellaro, S. 2008a, *GCN Circ.* 7163  
Valenti, S., D’Elia, V., Della Valle, M., Benetti, S., Chincarini,  
G., Mazzali, P. A., & Antonelli, L. A. 2008b, *GCN Circ.* 7221  
Waxman, E., Mészáros, P., & Campana, S. 2007, *ApJ*, 667, 351  
Xu, D., Zou, Y. C., & Fan, Y. Z. 2008, *ApJ*, arXiv:0801.4325,  
submitted

TABLE 2  
 LOG OF OPTICAL AND NEAR-INFRARED IMAGING OBSERVATIONS. FOR  
 THE *UBVRI* DATA, MAGNITUDES DO NOT INCLUDE THE ZEROPOINT  
 CALIBRATION ERROR OF 0.10, 0.03, 0.04, 0.03, AND 0.04 MAG,  
 RESPECTIVELY.

Epoch (UT)	Phase (days)	Filter	Magnitude	Instrument
Jan 11.26528	01.70082	<i>U</i>	18.60±0.02	NOT+StanCam
Jan 13.01426	03.44980	<i>U</i>	19.16±0.05	NOT+ALFOSC
Jan 15.22931	05.66485	<i>U</i>	19.40±0.05	NOT+ALFOSC
Jan 16.03116	06.46670	<i>U</i>	19.29±0.07	NOT+ALFOSC
Jan 17.25019	07.68573	<i>U</i>	19.19±0.07	NOT+ALFOSC
Jan 18.00103	08.43657	<i>U</i>	19.08±0.04	NOT+StanCam
Feb 01.06841	22.50395	<i>U</i>	19.11±0.04	NOT+ALFOSC
Feb 02.00892	23.44446	<i>U</i>	19.26±0.05	NOT+ALFOSC
Feb 04.03992	25.47546	<i>U</i>	19.45±0.04	NOT+ALFOSC
Feb 11.03650	32.47204	<i>U</i>	20.54±0.08	NOT+ALFOSC
Jan 11.04261	01.47815	<i>B</i>	19.00±0.01	NOT+StanCam
Jan 11.26873	01.70427	<i>B</i>	19.03±0.02	NOT+StanCam
Jan 13.01980	03.45534	<i>B</i>	19.21±0.02	NOT+ALFOSC
Jan 15.23748	05.67302	<i>B</i>	19.27±0.04	NOT+ALFOSC
Jan 16.03701	06.47255	<i>B</i>	19.11±0.01	NOT+ALFOSC
Jan 17.25617	07.69171	<i>B</i>	18.99±0.04	NOT+ALFOSC
Jan 18.00862	08.44416	<i>B</i>	18.99±0.05	NOT+StanCam
Jan 25.90236	16.33790	<i>B</i>	18.38±0.08	LT+RATCam
Jan 29.05104	19.48658	<i>B</i>	18.45±0.01	NOT+ALFOSC
Jan 30.98094	21.41648	<i>B</i>	18.48±0.07	NOT+ALFOSC
Feb 01.07844	22.51398	<i>B</i>	18.59±0.01	NOT+ALFOSC
Feb 02.01195	23.44749	<i>B</i>	18.67±0.01	NOT+ALFOSC
Feb 04.04304	25.47858	<i>B</i>	18.81±0.03	NOT+ALFOSC
Feb 11.04021	32.47575	<i>B</i>	19.55±0.03	NOT+ALFOSC
Feb 18.98034	40.41588	<i>B</i>	20.18±0.09	NOT+ALFOSC
Mar 01.09311	51.52865	<i>B</i>	20.51±0.03	NOT+ALFOSC
Mar 10.88157	61.31711	<i>B</i>	20.74±0.04	NOT+MOSCA
Apr 02.93574	84.37128	<i>B</i>	21.14±0.05	NOT+MOSCA
Jan 11.02120	01.45674	<i>V</i>	18.33±0.01	NOT+StanCam
Jan 11.27136	01.70690	<i>V</i>	18.35±0.06	NOT+StanCam
Jan 13.02744	03.46298	<i>V</i>	18.45±0.01	NOT+ALFOSC
Jan 15.24242	05.67796	<i>V</i>	18.13±0.05	NOT+ALFOSC
Jan 16.04183	06.47737	<i>V</i>	18.14±0.01	NOT+ALFOSC
Jan 17.26096	07.69650	<i>V</i>	17.99±0.02	NOT+ALFOSC
Jan 18.01366	08.44920	<i>V</i>	17.86±0.13	NOT+StanCam
Jan 20.02994	10.46548	<i>V</i>	17.75±0.03	NOT+StanCam
Jan 25.90873	16.34427	<i>V</i>	17.27±0.10	LT+RATCam
Jan 29.05856	19.49410	<i>V</i>	17.39±0.01	NOT+ALFOSC
Jan 30.19193	20.62747	<i>V</i>	17.39±0.02	NOT+ALFOSC
Jan 30.97634	21.41188	<i>V</i>	17.40±0.08	NOT+ALFOSC
Feb 01.08387	22.51941	<i>V</i>	17.45±0.01	NOT+ALFOSC
Feb 02.01399	23.44953	<i>V</i>	17.49±0.01	NOT+ALFOSC
Feb 04.04479	25.48033	<i>V</i>	17.59±0.01	NOT+ALFOSC
Feb 11.04238	32.47792	<i>V</i>	18.02±0.01	NOT+ALFOSC
Feb 18.98778	40.42332	<i>V</i>	18.53±0.04	NOT+ALFOSC
Mar 01.09818	51.53372	<i>V</i>	18.87±0.02	NOT+ALFOSC
Mar 10.88568	61.32122	<i>V</i>	19.06±0.05	NOT+MOSCA
Mar 17.86086	68.29640	<i>V</i>	19.24±0.08	NOT+ALFOSC
Apr 02.94851	84.38405	<i>V</i>	19.58±0.03	NOT+MOSCA
Apr 16.95106	98.38660	<i>V</i>	19.90±0.07	NOT+StanCam

TABLE 2  
(CONTINUED)

Epoch (UT)	Phase (days)	Filter	Magnitude	Instrument
Jan 11.00922	01.44476	<i>R</i>	17.94±0.01	NOT+StanCam
Jan 11.26190	01.69744	<i>R</i>	17.91±0.02	NOT+StanCam
Jan 11.30417	01.73971	<i>R</i>	17.94±0.02	VLT+FORs2
Jan 13.02367	03.45921	<i>R</i>	18.00±0.01	NOT+ALFOSC
Jan 15.24730	05.68284	<i>R</i>	17.80±0.01	NOT+ALFOSC
Jan 16.04659	06.48213	<i>R</i>	17.69±0.01	NOT+ALFOSC
Jan 17.26593	07.70147	<i>R</i>	17.54±0.01	NOT+ALFOSC
Jan 18.01774	08.45328	<i>R</i>	17.42±0.01	NOT+StanCam
Jan 20.04708	10.48262	<i>R</i>	17.16±0.04	NOT+StanCam
Jan 29.06847	19.50401	<i>R</i>	16.82±0.01	NOT+ALFOSC
Jan 30.21722	20.65276	<i>R</i>	16.80±0.02	NOT+ALFOSC
Jan 30.97162	21.40716	<i>R</i>	16.88±0.05	NOT+ALFOSC
Feb 01.08694	22.52248	<i>R</i>	16.84±0.01	NOT+ALFOSC
Feb 02.01603	23.45157	<i>R</i>	16.87±0.01	NOT+ALFOSC
Feb 04.04619	25.48173	<i>R</i>	16.92±0.01	NOT+ALFOSC
Feb 11.04420	32.47974	<i>R</i>	17.25±0.01	NOT+ALFOSC
Feb 18.99276	40.42830	<i>R</i>	17.62±0.01	NOT+ALFOSC
Mar 01.10190	51.53744	<i>R</i>	18.04±0.01	NOT+ALFOSC
Mar 02.12923	52.56477	<i>R</i>	18.07±0.02	NOT+ALFOSC
Mar 10.88805	61.32359	<i>R</i>	18.20±0.02	NOT+MOSCA
Mar 17.86648	68.30202	<i>R</i>	18.37±0.05	NOT+ALFOSC
Apr 02.95326	84.38880	<i>R</i>	18.72±0.04	NOT+MOSCA
Apr 16.94566	98.38120	<i>R</i>	19.01±0.04	NOT+StanCam
Jan 11.03211	01.46765	<i>I</i>	17.43±0.01	NOT+StanCam
Jan 11.27381	01.70935	<i>I</i>	17.40±0.01	NOT+StanCam
Jan 15.25279	05.68833	<i>I</i>	17.21±0.01	NOT+ALFOSC
Jan 16.05135	06.48689	<i>I</i>	17.09±0.01	NOT+ALFOSC
Jan 17.27084	07.70638	<i>I</i>	16.95±0.01	NOT+ALFOSC
Jan 18.02196	08.45750	<i>I</i>	16.79±0.01	NOT+StanCam
Jan 20.05173	10.48727	<i>I</i>	16.62±0.07	NOT+StanCam
Jan 29.07600	19.51154	<i>I</i>	16.18±0.01	NOT+ALFOSC
Jan 30.22517	20.66071	<i>I</i>	16.19±0.05	NOT+ALFOSC
Jan 30.99911	21.43465	<i>I</i>	16.16±0.04	NOT+ALFOSC
Feb 01.09031	22.52585	<i>I</i>	16.17±0.01	NOT+ALFOSC
Feb 02.01851	23.45405	<i>I</i>	16.18±0.01	NOT+ALFOSC
Feb 04.04764	25.48318	<i>I</i>	16.23±0.01	NOT+ALFOSC
Feb 11.04589	32.48143	<i>I</i>	16.45±0.01	NOT+ALFOSC
Feb 18.99647	40.43201	<i>I</i>	16.76±0.01	NOT+ALFOSC
Mar 01.07881	51.51435	<i>I</i>	17.09±0.01	NOT+ALFOSC
Mar 06.11299	56.54853	<i>I</i>	17.15±0.03	VLT+FORs1
Mar 10.89042	61.32596	<i>I</i>	17.16±0.04	NOT+MOSCA
Mar 17.87137	68.30691	<i>I</i>	17.48±0.06	NOT+ALFOSC
Apr 02.95712	84.39266	<i>I</i>	17.65±0.07	NOT+MOSCA
Apr 16.95661	98.39215	<i>I</i>	17.97±0.02	NOT+StanCam
Jan 12.555	02.99100	<i>J</i>	16.66±0.02	UKIRT+UFTI
Jan 14.598	05.03400	<i>J</i>	16.40±0.02	UKIRT+UFTI
Jan 15.457	05.89300	<i>J</i>	16.28±0.02	UKIRT+UFTI
Jan 17.645	08.08100	<i>J</i>	15.92±0.02	UKIRT+UFTI
Jan 21.004	11.44000	<i>J</i>	15.52±0.02	NOT+NOTCam
Jan 23.576	14.01200	<i>J</i>	15.47±0.02	UKIRT+UFTI
Feb 16.240	37.67600	<i>J</i>	15.54±0.02	UKIRT+WFCAM
Feb 25.295	46.73100	<i>J</i>	15.90±0.02	UKIRT+WFCAM
Mar 24.250	74.69000	<i>J</i>	16.85±0.02	UKIRT+WFCAM
Jan 12.555	02.99100	<i>H</i>	16.17±0.02	UKIRT+UFTI
Jan 14.598	05.03400	<i>H</i>	16.05±0.02	UKIRT+UFTI
Jan 15.457	05.89300	<i>H</i>	15.91±0.02	UKIRT+UFTI
Jan 17.645	08.08100	<i>H</i>	15.55±0.02	UKIRT+UFTI
Jan 21.004	11.44000	<i>H</i>	15.13±0.02	NOT+NOTCam
Jan 23.576	14.01200	<i>H</i>	15.05±0.02	UKIRT+UFTI
Feb 16.240	37.67600	<i>H</i>	15.05±0.02	UKIRT+WFCAM
Feb 25.295	46.73100	<i>H</i>	15.32±0.02	UKIRT+WFCAM
Mar 24.250	74.69000	<i>H</i>	16.07±0.02	UKIRT+WFCAM
Jan 12.555	02.99100	<i>K</i>	15.99±0.02	UKIRT+UFTI
Jan 14.598	05.03400	<i>K</i>	15.71±0.02	UKIRT+UFTI
Jan 15.457	05.89300	<i>K</i>	15.55±0.02	UKIRT+UFTI
Jan 17.645	08.08100	<i>K</i>	15.20±0.02	UKIRT+UFTI
Jan 21.004	11.44000	<i>K</i>	14.83±0.02	NOT+NOTCam
Jan 23.576	14.01200	<i>K</i>	14.72±0.02	UKIRT+UFTI
Feb 16.240	37.67600	<i>K</i>	14.68±0.02	UKIRT+WFCAM
Feb 25.295	46.73100	<i>K</i>	14.98±0.02	UKIRT+WFCAM
Mar 24.250	74.69000	<i>K</i>	15.75±0.02	UKIRT+WFCAM